Electromagnetic control and improvement of nonclassicality in a strongly coupled single-atom cavity-QED system

Y. F. Han,[1,2] C. J. Zhu,[1,*] X. S. Huang,[2] and Y. P. Yang[1,†]

[1]*MOE Key Laboratory of Advanced Micro-Structured Materials, School of Physics Science and Engineering, Tongji University, Shanghai 200092, China*

[2]*School of Mathematics and Physics, Anhui University of Technology, Ma'anshan 243032, China*

(Received 11 May 2018; published 27 September 2018)

We present a proposal to control and improve the nonclassicality of photons in a single-atom cavity-QED system with a strong coupling strength, where the atom is directly driven by external fields. Exploring the eigenvalues and the corresponding eigenstates of the system, we show that the dressed states can be optically manipulated by changing the control field intensity. In particular, tuning the control field frequency to be resonant with the one-photon excitation state, we show that the nonclassicality of cavity photons arising from the two-photon blockade can be actively controlled. We also show that there exists a magic control field Rabi frequency at which the two-photon blockade phenomenon can be significantly improved. The work presented here provides an optical method to control the statistical features of the cavity field that could find utility in nonclassical light generation, photon gateway operation, and exotic quantum-state generation.

DOI: 10.1103/PhysRevA.98.033828

I. INTRODUCTION

Nonclassical properties of the optical field, such as squeezing, antibunching, and sub-Poissonian photon statistics, have been intensively studied in modern quantum optics [1,2]. Using these features of the nonclassical optical field, many applications including high-precision optical measurements, optical imaging, optical information processing, and high-fidelity optical communications can be achieved based on the possibility of overcoming the so-called standard quantum limit [3–9]. The generation of nonclassical light remains an open question, despite many attempts to control nonclassical optical fields.

In general, the field correlation function is an effective quantity to characterize the nonclassical optical field which is defined by $g^{(2)}(\tau) = \langle \hat{I}(t)\hat{I}(t+\tau)\rangle / \langle \hat{I}(t)\rangle^2$ [10,11]. It reflects the probability of detecting one photon at time $t+\tau$ provided that one was detected at time t. According to the Schwartz inequality, the optical field is classical if the field correlation function $g^{(2)}(0) > g^{(2)}(\tau)$. The violation of this condition represents a nonclassical optical field such as antibunching [$g^{(2)}(0) < g^{(2)}(\tau)$] and a sub-Poissonian distribution with $g^{(2)}(0) < 1$.

In the past decade, antibunching photons have been theoretically and experimentally studied in cavity quantum electrodynamics (QED) systems based on the two-photon blockade phenomenon [12]. In a single-atom cavity-QED system, antibunching photons with a sub-Poissonian distribution [$g^{(2)}(0) < g^{(2)}(\tau)$ and $g^{(2)}(0) < 1$] can be observed since $N > 1$ photon transitions are blockaded due to vacuum Rabi splitting. To date, the realization of antibunching photons with a sub-Poissonian distribution has been reported in many configurations, including the cavity-QED system [13,14], artificial atoms on a chip [15,16], a cavity with Kerr nonlinearity [17–19], and superconducting circuits [20,21].

Using electromagnetically induced transparency (EIT) based on the quantum interference effect [22–24], it is possible to control the nonclassicality of an optical field. By merging the EIT configuration with the cavity-QED system, two-photon blockade can be enhanced [19,25] and many interesting phenomena have been theoretically proposed and experimentally demonstrated, including slow light propagation [26,27], cavity cooling [28–30], cross phase modulation and quantum phase gate operation [31–33], the all-optical switch and transistor [34–38], and quantum information processing [39,40]. Besides, a cavity-assisted Rydberg-atom EIT phenomenon in a high-finesse optical cavity has been experimentally demonstrated [41], and Wu *et al.* explore the possibility of generating and controlling optical frequency combs in a cavity EIT system [42].

In this work, we present some results for electromagnetic control and improvement of the nonclassicality of cavity photons in a strongly coupled single-atom cavity-QED system, where the atom is directly driven by a probe field and a control field, forming a Λ-type configuration. Compared with cavity driving, atom driving gives a larger optical nonlinearity, resulting in the improvement of two-photon blockade [43], observation of three-photon blockade [14], and realization of the hyperradiance phenomenon [44,45]. Even if the driving field is strong, the second-order correlation function can be very small. This scheme is motivated by work on the atom-driven system and cavity-EIT configuration, where the nonclassicality of cavity photons can be controlled using EIT technique [14,25]. However, differently from early works on the cavity-EIT system [25,46], we consider the atom-driven case, and the frequency of the control field is tuned to be

*cjzhu@tongji.edu.cn
†yang_yaping@tongji.edu.cn

 ©2018 American Physical Society

resonant with the one-photon excitation state rather than the cavity. We show that our scheme not only can be used to control the nonclassicality of cavity photons but also exhibits many advantages that the cavity-EIT system does not have. For example, by exploring the well-known ladder-type eigenstates, we find that the one-photon excitation state will be split into a doublet, and the splitting width is nearly proportional to the control field Rabi frequency. We also show that there exists a *magic* control field intensity where the second-order correlation function decreases to a very small value, but the mean photon number is reasonable. Compared with the cavity-EIT scheme, we show that the two-photon blockade effect can be significantly enhanced in our scheme, resulting in antibunching photons leaking from the cavity. Based on these features, we show that our scheme is a good candidate for controlling the nonclassicality of cavity photons by adjusting the external control field intensity, which provides an optical knob for changing the statistic features of the cavity field.

The paper is arranged as follows. In Sec. II, we present the theoretical model of this three-level atom-cavity system. In Sec. III, we give a detailed discussion of the eigenvalues and the corresponding eigenstates of the system. In Secs. IV and V, we study the cavity excitation spectrum and explore the nonclassicality of the cavity field in the case of $\Delta_L = 0$ and $\Delta_L = -g$, respectively. Moreover, the role of the probe field is discussed. A summary of the main results is given in Sec. VI.

II. THEORETICAL MODEL

To begin with, we consider a three-level Λ-type atom strongly coupled to a single-mode cavity of wavelength λ_c (see Fig. 1). In experiments, these three states can be chosen as $|g\rangle = |5S_{1/2}, F = 1\rangle$, $|e\rangle = |5P_{1/2}, F' = 1\rangle$, and $|m\rangle = |5S_{1/2}, F = 2\rangle$ of the ^{87}Rb atom [47,48]. A probe field with Rabi frequency η couples the $|g\rangle \leftrightarrow |e\rangle$ transition, and a control field with Rabi frequency Ω_L couples the $|m\rangle \leftrightarrow |e\rangle$ transition.

Under the rotating-wave and electric dipole approximations, the Hamiltonian of this single-atom cavity-QED system can be written as

$$H = \Delta_e\sigma_{ee} + \Delta_m\sigma_{mm} + \Delta_c a^\dagger a + g(a\sigma_{eg} + a^\dagger\sigma_{ge}) + \Omega_L(\sigma_{em} + \sigma_{me}) + \eta(\sigma_{eg} + \sigma_{ge}), \quad (1)$$

where a and $a^\dagger$ are the annihilation and creation operators of the cavity field, and $\sigma_{ij} = |i\rangle\langle j|$ $(i, j = g, e, m)$ are the atomic raising and lowering operators for $i \neq j$ and the atomic population operators for $i = j$. The detunings are defined as $\Delta_c = \omega_c - \omega_p$, $\Delta_e = (\omega_e - \omega_g) - \omega_p$, and $\Delta_m = \Delta_e - \Delta_L$, with the control field detuning $\Delta_L = (\omega_e - \omega_m) - \omega_L$. Here, the energy of the $|j\rangle$ state is $\hbar\omega_j$ $(j = g, e, m)$, $\omega_c = 2\pi/\lambda_c$ is the cavity-mode frequency, and $\omega_{p(L)}$ is the angular frequency of the probe (control) field. Assuming that $\omega_c = \omega_e - \omega_g$, we can take $\Delta_p \equiv \Delta_c = \Delta_e$ in the following for simplicity.

In general, the properties of the entire system can be obtained by numerically solving the master equation, i.e.,

$$\frac{d}{dt}\rho = -\frac{i}{\hbar}[H, \rho] + \mathcal{L}_{\text{atom}}(\rho) + \mathcal{L}_{\text{cavity}}(\rho), \quad (2)$$

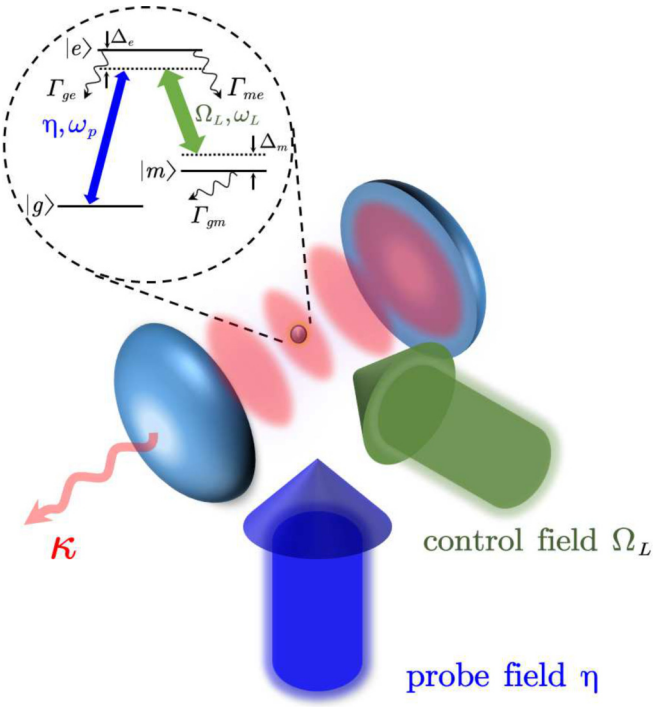

FIG. 1. System configuration of a three-level Λ-type atom strongly coupled to a single-mode cavity of wavelength λ_c. A probe field η with angular frequency ω_p drives the $|g\rangle \leftrightarrow |e\rangle$ transition, and a control field Ω_L with angular frequency ω_L drives the $|m\rangle \leftrightarrow |e\rangle$ transition. Here, the cavity decay rate is denoted κ. Γ_{ge} and Γ_{me} represent the spontaneous decay rates from the $|e\rangle$ state to the $|g\rangle$ and $|m\rangle$ states, respectively. The decay rate of the metastable state $|m\rangle$ is denoted Γ_{gm}. $\Delta_e = (\omega_e - \omega_g) - \omega_p$ and $\Delta_m = (\omega_m - \omega_g) - (\omega_p - \omega_L)$ are the detunings of the $|e\rangle$ and $|m\rangle$ states, respectively.

where ρ is the density operator of the single-atom cavity-QED system, and $\mathcal{L}_{\text{atom}}(\rho)$ and $\mathcal{L}_{\text{cavity}}(\rho)$ are the Liouvillian operators for the atomic decay and cavity decay, respectively, which are given by

$$\begin{aligned}\mathcal{L}_{\text{atom}}(\rho) = {} & \Gamma_{ge}(2\sigma_{eg}^\dagger\rho\sigma_{eg} - \sigma_{eg}\sigma_{eg}^\dagger\rho - \rho\sigma_{eg}\sigma_{eg}^\dagger) \\ & + \Gamma_{me}(2\sigma_{em}^\dagger\rho\sigma_{em} - \sigma_{em}\sigma_{em}^\dagger\rho - \rho\sigma_{em}\sigma_{em}^\dagger) \\ & + \Gamma_{gm}(2\sigma_{mg}^\dagger\rho\sigma_{mg} - \sigma_{mg}\sigma_{mg}^\dagger\rho - \rho\sigma_{mg}\sigma_{mg}^\dagger)\end{aligned}$$

and

$$\mathcal{L}_{\text{cavity}}(\rho) = \kappa(2a\rho a^\dagger - a^\dagger a\rho - \rho aa^\dagger),$$

with Γ_{ij} $(i, j = g, e, m)$ being the decay rate from the $|j\rangle$ to the $|i\rangle$ state and κ being the decay rate of the cavity.

III. EIGENVALUES AND DRESSED-STATE PICTURE

For any quantum system, it is helpful to study the eigenvalues and the corresponding eigenstates of the system, so that the physical mechanism of this system can be understood very well. Assuming that $\eta = \Delta_p = 0$ [49], the Hamiltonian can be rewritten in a new set of basis $\{|g, n\rangle, |+, n-1\rangle, |-, n-1\rangle\}$, with n being the number of photons in the cavity and $|\pm, n-1\rangle = (|m, n-1\rangle \pm |e, n-1\rangle)/\sqrt{2}$. Therefore, in the n-photon space, the Hamiltonian can be

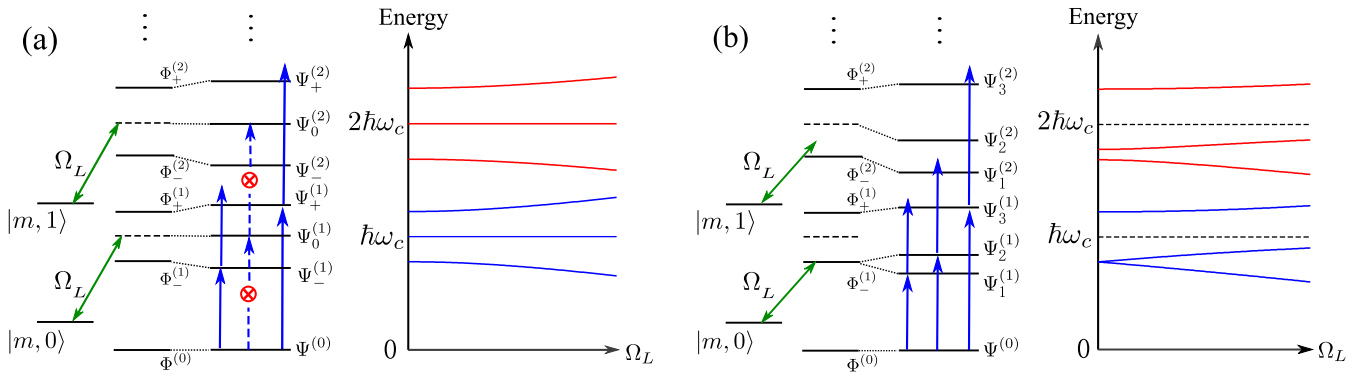

FIG. 2. Dressed-state structure and eigenvalues of this single-atom cavity-QED system with $\Delta_L = 0$ (a) and $\Delta_L = -g$ (b). Solid arrowed blue lines represent the allowed transitions for the probe field, and dashed arrowed lines represent the forbidden transitions. Here, eigenvalues are obtained by numerically solving Eq. (3) with $g = 20$.

expressed as [25,50]

$$H^{(n)} = \begin{pmatrix} 0 & g\sqrt{n/2} & -g\sqrt{n/2} \\ g\sqrt{n/2} & \Omega_L - \Delta_L/2 & -\Delta_L/2 \\ -g\sqrt{n/2} & -\Delta_L/2 & -\Omega_L - \Delta_L/2 \end{pmatrix}. \tag{3}$$

In the case of $\Delta_L = 0$, the eigenvalues of the Hamiltonian $H^{(n)}$ can be solved analytically, yielding $\lambda_0^{(n)} = 0$ and $\lambda_\pm^{(n)} = \pm\sqrt{\Omega_L^2 + ng^2}$. The corresponding eigenstates are given by

$$\Psi_0^{(n)} = \mathcal{N}_0^{(n)}\left(|g,n\rangle - \frac{g\sqrt{n}}{\Omega_L}|m,n-1\rangle\right) \tag{4}$$

and

$$\Psi_\pm^{(n)} = \mathcal{N}_\pm^{(n)}\left(|g,n\rangle + \frac{g\sqrt{n/2}}{\lambda_\pm^{(n)} - \Omega_L}|+,n-1\rangle - \frac{g\sqrt{n/2}}{\lambda_\pm^{(n)} + \Omega_L}|-,n-1\rangle\right), \tag{5}$$

where $\mathcal{N}_0^{(n)}$ and $\mathcal{N}_\pm^{(n)}$ are the normalization factors. Clearly, the eigenstates $\Psi_0^{(n)}$ are the intracavity dark states which cannot be excited. Then the remaining eigenstates form a ladder of energy levels, which are arranged in doublets. The splitting between doublets depends on the control field Rabi frequency Ω_L and the quantum number n [see Fig. 2(a), right], which is not increased linearly with respect to the control field Rabi frequency if the coupling strength is high. These results can also be explained by decomposing the system into two subsystems. One is the subsystem consisting of the cavity and a two-level atom with the $|g\rangle$ and $|e\rangle$ states, and the other is the subsystem consisting of the control field and $|m\rangle$ state. As we all know, the first subsystem has been studied extensively; it forms a ladder of doublet levels with energy splitting $2g\sqrt{n}$ [see Fig. 2(a), left]. The corresponding eigenvalues and eigenstates are given by $\Lambda_\pm^{(n)} = g\sqrt{n}$ and $\Phi_\pm^{(n)} = (\pm|g,n\rangle + |e,n-1\rangle)/\sqrt{2}$, respectively. Therefore, in the case of detuning $\Delta_L = 0$, the energies of $\Phi_\pm^{(n)}$ states are shifted since the control field is far off-resonant with each state [see Fig. 2(a)].

When the probe field frequency is tuned to one of the first manifold dressed states, the absorption of a second photon at the same frequency is blocked because transitions to two-photon excitation states are detuned from resonance under the strong-coupling condition, resulting in the well-known two-photon blockade phenomenon. With an increase in the control field Rabi frequency, the energy of the dressed states is shifted so that the probe field frequency to realize two-photon blockade is modified. We also show that there exists a magic control field Rabi frequency where the second-order correlation function goes to a smaller value and the two-photon blockade effect is enhanced (see Sec. IV).

Likewise, the control field can also be tuned resonant with the $|m,0\rangle \leftrightarrow \Phi_-^{(1)}$ transition by choosing the detuning $\Delta_L = -g$. As a result, the $\Phi_-^{(1)}$ state is split into a doublet, but the $\Phi_+^{(1)}$ state undergoes an energy shift due to the off-resonant coupling [see Fig. 2(b), left]. Directly solving the eigenvalues of the Hamiltonian given in Eq. (3), we show that eigenvalues with photon number $n = 1,\ 2$ change with the control field Rabi frequency Ω_L in Fig. 2(b), right. It is clear to see that the numerical results match very well with the analysis based on the dressed states. Manipulating the dressed states by changing the control field Rabi frequency, it is possible to change the nonclassicality of cavity photons and the frequency of the probe field to achieve two-photon blockade. Differently from the case of $\Delta_L = 0$, the state $\Phi_-^{(1)}$ is resonantly coupled by the control field so that the width of the energy splitting is nearly proportional to the control field Rabi frequency [see blue curves in Fig. 2(b)]. However, other states are shifted nonlinearly with respect to the control field Rabi frequency because of the far-off-resonant coupling. These features may result in a significant improvement in the two-photon blockade phenomenon if the magic control field Rabi frequency is utilized (see Sec. V).

IV. THE CASE OF $\Delta_L = 0$

Before studying the nonclassicality of the cavity field, we calculate the mean photon number $n_{\rm cav} = \langle a^\dagger a\rangle$ in the cavity by numerically solving Eq. (2), which directly reflects the energy shifts of each eigenstate. In Fig. 3(a), we plot the mean photon number $n_{\rm cav}$ as a function of the normalized

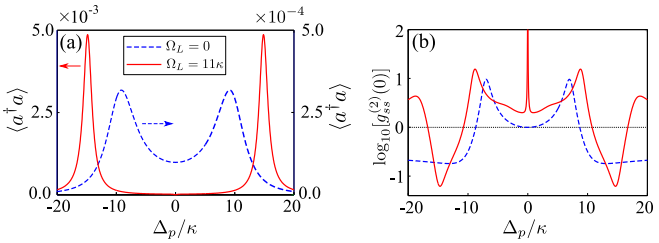

FIG. 3. (a) Mean photon number $\langle a^\dagger a\rangle$ and (b) steady-state second-order photon-photon correlation function $\log_{10}[g^{(2)}_{ss}(0)]$ as a function of the normalized detuning Δ_p/κ for the probe field. The control field is taken as $\Omega_L = 0$ Hz (dashed blue curve) and 11.0κ (solid red curve), respectively. Other system parameters are chosen as $\Delta_L = 0$, $\Gamma_{ge} = \Gamma_{me} = 1.5\kappa$, $\Gamma_{gm} = 5 \times 10^{-4}\kappa$, $g = 10\kappa$, and $\eta = 0.1\kappa$. The dash-dotted line in (b) indicates the condition $\log_{10}[g^{(2)}_{ss}(0)] = 0$ [i.e., $g^{(2)}_{ss}(0) = 1$].

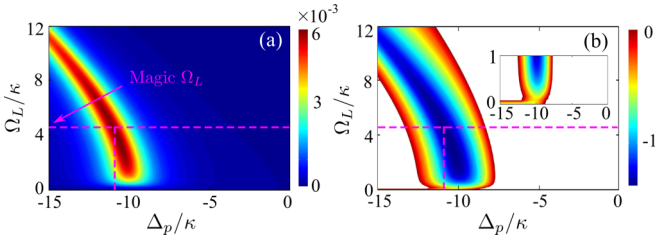

FIG. 4. (a) Mean photon number n_{cav} and (b) steady-state second-order field correlation function $\log_{10}[g^{(2)}_{ss}(0)]$ as functions of the normalized detuning Δ_p/κ and control field Rabi frequency Ω_L/κ, respectively. The horizontal dashed pink line indicates the magic control field Rabi frequency, where a specific probe field detuning (indicated by the vertical dashed pink line) can be chosen to realize an improved two-photon blockade phenomenon with the reasonable photon number. The white area in (b) denotes the regime where $\log_{10}[g^{(2)}_{ss}(0)] > 0$.

detuning Δ_p/κ for the probe field. Here, we choose the control field Rabi frequencies $\Omega_L/\kappa = 0$ (dashed blue curve) and 11.0 (solid red curve), respectively. Other system parameters are chosen as $\Delta_L = 0$, $\Gamma_{ge} = \Gamma_{me} = 1.5\kappa$, $\Gamma_{gm} = 5 \times 10^{-4}\kappa$, $g = 10\kappa$, and $\eta = 0.1\kappa$ [47,51]. In the absence of the control field (i.e., $\Omega_L = 0$ Hz), we can observe two peaks (see the dashed blue curve) at $\Delta_p = \pm g$ in the cavity excitation spectrum, which correspond to two one-photon transitions, i.e., $\Phi^{(0)}_0 \to \Phi^{(1)}_\pm$. In the presence of the control field, however, the position and amplitude of these two resonant peaks change greatly as the eigenvalues and eigenstates of the system are modified by the control field. As shown in Fig. 2(a), we can observe a larger energy splitting between two peaks (i.e., $2\sqrt{g^2 + \Omega_L^2}$; see the solid red curve), and the corresponding mean photon number also increases significantly. It is noteworthy that high-order transitions are too weak to be observed since the multiphoton ($n \geqslant 2$) transitions are far off-resonant, which results in the two-photon blockade phenomenon.

To characterize this interesting phenomenon, we calculate the equal-time, second-order field correlation function $g^{(2)}_{ss}(0) = \langle a^\dagger(0)a^\dagger(0)a(0)a(0)\rangle / \langle a^\dagger(0)a(0)\rangle^2$ under the steady-state condition. As shown in Fig. 3(b), the second-order correlation function $g^{(2)}_{ss}(0) < 1$ for the peaks in the cavity excitation spectrum (corresponding to one-photon transitions), which is evidence of the two-photon blockade phenomenon. Another key feature of this system is the presence of strong photon bunching behavior [$g^{(2)}_{ss}(0) \gg 1$] at the central frequency (i.e., $\Delta_p = 0$). In the absence of the control field, the probe field is off-resonant with all states so that the quantum property of the cavity field is the same as that of the probe field, and the second-order correlation function $g^{(2)}_{ss}(0) = 1$ (i.e., a coherent field). When the control field is turned on, additional states $\Psi^{(n)}_0$ appear and can be excited via multiphoton transition processes, resulting in classical field generation with superbunching behavior, i.e., $g^{(2)}_{ss}(0) \gg 1$.In Figs. 4(a) and 4(b), we plot the mean photon number n_{cav} and the steady-state second-order field correlation function $\log_{10}[g^{(2)}_{ss}(0)]$ as functions of the normalized detuning Δ_p/κ and control field Rabi frequency Ω_L/κ, respectively. Here, the system parameters are the same as those used in Fig. 3, and we just consider the case of blue detuning (i.e., $\Delta_p < 0$) due to the symmetry of the system. As shown in Fig. 4(a), the width of the energy-level splitting almost increases linearly as the intensity of the control field increases. Correspondingly, the second-order field correlation function, strongly dependent on the cavity photon excitation, varies significantly [see Fig. 4(b)]. In particular, there exists a magic control field intensity (indicated by the horizontal dashed pink line) to obtain the minimum of the second-order field correlation function. As a result, an improved two-photon blockade phenomenon with a reasonable photon number can be achieved by choosing a specific probe field detuning indicated by the vertical dashed pink line. For example, at the detuning $\Delta_p/\kappa = -10.8$, one obtains $g^{(2)}_{ss}(0) \approx 0.04$ and $n_{cav} \approx 0.006$ with $\Omega_L/\kappa = 4.5$.

V. THE CASE OF $\Delta_L = -g$

Now, we consider the case of $\Delta_L = -g$, where the control field is tuned resonant with the $\Phi^{(1)}_-$ state shown in Fig. 2(b). In this case, the $\Phi^{(1)}_-$ state is split into two separate states labeled $\Psi^{(1)}_1$ and $\Psi^{(1)}_2$, respectively. Because of this large detuning Δ_L, the coupling between the control field and other states in the cavity-QED system can be safely neglected. Therefore, there exist three resonant peaks in the cavity excitation spectrum as shown in Fig. 5(a), corresponding to the $|\Psi_0\rangle \leftrightarrow |\Psi^{(1)}_1\rangle$, $|\Psi_0\rangle \leftrightarrow |\Psi^{(1)}_2\rangle$, and $|\Psi_0\rangle \leftrightarrow |\Psi^{(1)}_3\rangle$ transitions, respectively. Here, the control field is taken as $\Omega_L/\kappa = 9.0$ (solid red curve), and other system parameters are the same as those used in Fig. 3. It is noted that the mean photon number in the cavity is significantly enhanced compared with the case of $\Omega_L = 0$. In Fig. 5(b), we plot the steady-state second-order field correlation function $g^{(2)}_{ss}(0)$ as a function of the normalized detuning Δ_p/κ with the control field Rabi frequencies $\Omega_L/\kappa = 0$ and 9, respectively. Clearly, in the presence of the control field, superbunching behavior [i.e., $g^{(2)}_{ss}(0) \gg 1$] can be observed at $\Delta_p = -g$, where $g^{(2)}_{ss}(0) < 1$ if the control field is turned off. In addition, the second-order field correlation function drops quickly at a frequency near the middle peak in the cavity excitation spectrum, which provides the possibility of achieving a significant improvement in the

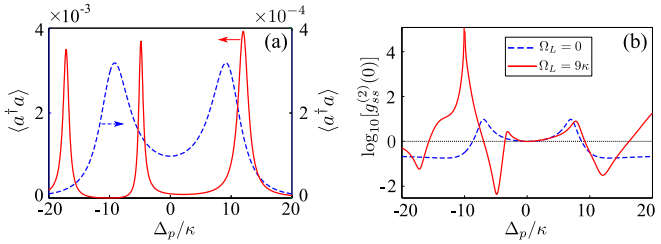

FIG. 5. (a) Mean photon number $\langle a^\dagger a\rangle$ and (b) steady-state second-order field correlation function $\log_{10}[g^{(2)}_{ss}(0)]$. Here, we choose $\Delta_L = -g$ and the control field Rabi frequencies are chosen as $\Omega_L/\kappa = 0$ (dashed blue curves) and 9.0 (solid red curve), respectively. Other system parameters are the same as those used in Fig. 3. The dash-dotted line in (b) corresponds to $\log_{10}[g^{(2)}_{ss}(0)] = 0$ [i.e., $g^{(2)}_{ss}(0) = 1$].

two-photon blockade phenomenon.Figures 6(a) and 6(b) show the mean photon number n_{cav} and the steady-state second-order field correlation function $\log_{10}[g^{(2)}_{ss}(0)]$ as functions of the normalized control field Rabi frequency Ω_L/κ and detuning Δ_p/κ, which is chosen near the middle peak. As shown in Fig. 6(a), the width of the energy splitting caused by the control field is almost proportional to the control field Rabi frequency. In particular, we can obtain a magic control field intensity indicated by the horizontal dashed pink line, where the two-photon blockade phenomenon can be significantly improved when a specific probe field detuning is chosen (indicated by the vertical line). According to our numerical calculation, the mean photon number $n_{cav} \approx 0.004$ and the second-order field correlation function $g^{(2)}_{ss}(0) \approx 0.004$ at $\Delta_p/\kappa = -4.8$. Therefore, a nonclassical field with antibunching behavior is generated in this three-level atom-cavity QED system. In Figs. 6(c) and 6(d), we choose the detuning Δ_p near the right peak in the cavity excitation spectrum. As shown in

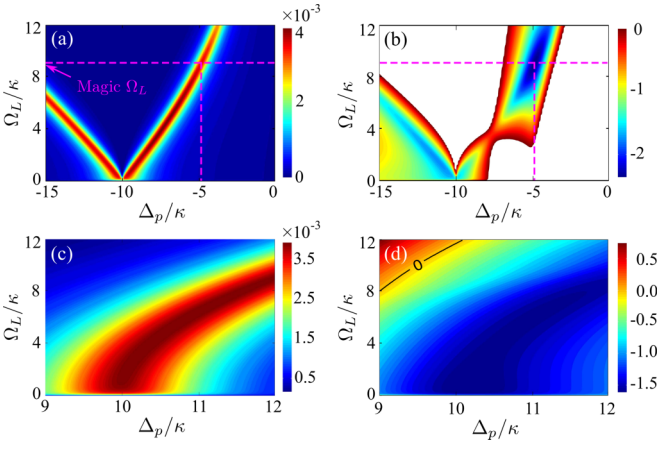

FIG. 6. (a), (c) Mean photon number n_{cav} and (b), (d) steady-state second-order field correlation function $\log_{10}[g^{(2)}_{ss}(0)]$. The horizontal dashed pink line in (a) and (b) indicates the magic control field Rabi frequency, where a specific probe field detuning (indicated by the vertical dashed pink line) can be chosen to achieve a significantly improved two-photon blockade phenomenon. The white areas in (b) denote the regime of $g^{(2)}_{ss}(0) > 1$. The black curve in (d) indicates the equal attitude line of $\log_{10}[g^{(2)}_{ss}(0)] = 0$ [i.e., $g^{(2)}_{ss}(0) = 1$].

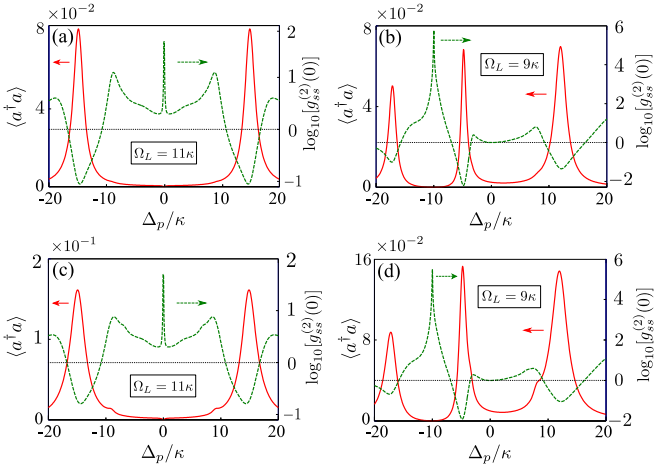

FIG. 7. The mean photon number $\langle a^\dagger a\rangle$ (solid red curve) and steady-state second-order field correlation function $\log_{10}[g^{(2)}_{ss}(0)]$ (dashed green curve) are plotted as a function of the normalized detuning Δ_p/κ with (a), (b) $\eta = 0.5\kappa$ and (c), (d) $\eta = 1.0\kappa$. In (a) and (c) we choose $\Delta_L = 0$; in (b) and (d), $\Delta_L = -g$. Other system parameters are the same as those used in Fig. 3, and the dash-dotted line corresponds to $\log_{10}[g^{(2)}_{ss}(0)] = 0$ [i.e., $g^{(2)}_{ss}(0) = 1$].

Fig. 6(d), the statistical feature of the cavity field changes from antibunching to superbunching with an increasing control field intensity. Correspondingly, the property of the photons leaking from the cavity can be controlled from quantum to classic by adjusting the control field.

VI. DISCUSSION AND CONCLUSION

Before closing, we consider the influence of the probe field intensity on the mean photon number and the field correlation function. In Fig. 7, we plot the mean photon number $\langle a^\dagger a\rangle$ and the steady-state second-order field correlation function $g^{(2)}_{ss}(0)$ as a function of the normalized detuning Δ_p/κ with $\eta = 0.5\kappa$ [Figs. 7(a) and 7(b)] and $\eta = 1.0\kappa$ [Figs. 7(c) and 7(d)]. In Figs. 7(a) and 7(c) we choose $\Delta_L = 0$, but $\Delta_L = -g$ in Figs. 7(b) and 7(d). Obviously, the mean photon number can be significantly enhanced by increasing the probe field intensity so that photons leaking from the cavity can be detected in experiments. As shown in Figs. 7(a) and 7(c), the mean photon number can be increased to 0.16, but the value of the second-order field correlation function changes slightly. For example, we can obtain $g^{(2)}_{ss}(0) \approx 0.1$ for $\eta = 0.5\kappa$ and $g^{(2)}_{ss}(0) \approx 0.16$ for $\eta = 1.0\kappa$. Furthermore, the photon blockade phenomenon can also be improved in the case of $\Delta_L = -g$, even if a strong probe field intensity is used [see Figs. 7(b) and 7(d)]. It is found that the mean photon number can reach up to 0.15, and the second-order correlation function is about 0.012, which can be recognized as a complete photon blockade in experiments.

In conclusion, we have shown that the quantum properties of the cavity field in a strongly coupled three-level atom-cavity QED system can be actively controlled by using an electromagnetic field. This arises from the change in the dressed-state structure of the system formed by the interacting fields and atom. We show that the dressed-state structure

and allowed transitions strongly depend on the control field intensity and frequency. We also show that, in the case of $\Delta_L = 0$, the two-photon blockade phenomenon can be enhanced and the superbunching behavior of the cavity field can be measured in this atom-cavity QED system. In the case of $\Delta_L = -g$, we show that the significantly improved two-photon blockade phenomenon can be observed if a magic control field intensity is chosen. We further show that the property of the cavity field can be controlled from quantum to classic by increasing the control field intensity. Compared with the traditional cavity-EIT scheme (i.e., $\Delta_L = 0$), our scheme presented here (i.e., $\Delta_L = -g$) is a good candidate for the realization of nonclassical light generation, optical controlled quantum gate operation, and exotic quantum-state preparation.

ACKNOWLEDGMENTS

We thank G. S. Agarwal at Texas A&M university for stimulating discussions. We acknowledge the National Key Basic Research Special Foundation (Grant No. 2016YFA0302800); the Shanghai Science and Technology Committee (Grant No. 18JC1410900); The National Natural Science Foundation of China (Grants No. 11774262, No. 11474003, No. 11504003, and No. 61675006); and the Anhui Provincial Natural Science Foundation (Grants No. 1408085MA19 and No. 1608085ME102).

[1] M. O. Scully and M. S. Zubairy, *Quantum Optics* (Cambridge University Press, Cambridge, UK, 1997).
[2] G. S. Agarwal, *Quantum Optics* (Cambridge University Press, Cambridge, UK, 2012).
[3] H.-A. Bachor and T. C. Ralph, *A Guide to Experiments in Quantum Optics* (Wiley, New York, 2004).
[4] M. Xiao, L.-A. Wu, and H. J. Kimble, Phys. Rev. Lett. **59**, 278 (1987).
[5] N. Treps, U. Andersen, B. Buchler, P. K. Lam, A. Maitre, H.-A. Bachor, and C. Fabre, Phys. Rev. Lett. **88**, 203601 (2002).
[6] P. Grangier, R. E. Slusher, B. Yurke, and A. LaPorta, Phys. Rev. Lett. **59**, 2153 (1987).
[7] E. Polzik, J. Carri, and H. Kimble, Appl. Phys. B **55**, 279 (1992).
[8] F. Marin, A. Bramati, V. Jost, and E. Giacobino, Opt. Commun. **140**, 146 (1997).
[9] Y. Yamamoto, S. Machida, S. Saito, N. Imoto, T. Yanagawa, M. Kitagawa, and G. Björk, Prog. Opt. **28**, 87 (1990).
[10] R. J. Brecha, P. R. Rice, and M. Xiao, Phys. Rev. A **59**, 2392 (1999).
[11] J. P. Clemens and P. R. Rice, Phys. Rev. A **61**, 063810 (2000).
[12] K. M. Birnbaum, A. Boca, R. Miller, A. D. Boozer, T. E. Northup, and H. J. Kimble, Nature **436**, 87 (2005).
[13] B. Dayan, Science **319**, 1062 (2008).
[14] C. Hamsen, K. N. Tolazzi, T. Wilk, and G. Rempe, Phys. Rev. Lett. **118**, 133604 (2017).
[15] A. Faraon, I. Fushman, D. Englund, N. Stoltz, P. Petroff, and J. Vučković, Nat. Phys. **4**, 859 (2008).
[16] A. Reinhard, T. Volz, M. Winger, A. Badolato, K. J. Hennessy, E. L. Hu, and A. Imamoğlu, Nat. Photon. **6**, 93 (2012).
[17] A. Imamoğlu, H. Schmidt, G. Woods, and M. Deutsch, Phys. Rev. Lett. **79**, 1467 (1997).
[18] S. Rebić, S. Tan, A. Parkins, and D. Walls, J. Opt. B: Quantum Semiclass. Opt. **1**, 490 (1999).
[19] S. Rebić, A. S. Parkins, and S. M. Tan, Phys. Rev. A **65**, 063804 (2002).
[20] C. Lang, D. Bozyigit, C. Eichler, L. Steffen, J. M. Fink A. A. Abdumalikov, M. Baur, S. Filipp, M. P. da Silva, A. Blais, and A. Wallraff, Phys. Rev. Lett **106**, 243601 (2011).
[21] A. J. Hoffman, S. J. Srinivasan, S. Schmidt, L. Spietz, J. Aumentado, H. E. Türeci, and A. A. Houck, Phys. Rev. Lett. **107**, 053602 (2011).
[22] K.-J. Boller, A. Imamoğlu, and S. E. Harris, Phys. Rev. Lett. **66**, 2593 (1991).
[23] M. Fleischhauer, A. Imamoglu, and J. P. Marangos, Rev. Mod. Phys. **77**, 633 (2005).
[24] M. Mücke, E. Figueroa, J. Bochmann, C. Hahn, K. Murr, S. Ritter, C. J. Villas-Boas, and G. Rempe, Nature **465**, 755 (2010).
[25] J. A. Souza, E. Figueroa, H. Chibani, C. J. Villas-Boas, and G. Rempe, Phys. Rev. Lett. **111**, 113602 (2013).
[26] J. Zhang, G. Hernandez, and Y. Zhu, Opt. Lett. **33**, 46 (2008).
[27] G. Nikoghosyan and M. Fleischhauer, Phys. Rev. Lett. **105**, 013601 (2010).
[28] T. Kampschulte, W. Alt, S. Brakhane, M. Eckstein, R. Reimann, A. Widera, and D. Meschede, Phys. Rev. Lett. **105**, 153603 (2010).
[29] M. Bienert and G. Morigi, New J. Phys. **14**, 023002 (2012).
[30] T. Kampschulte, W. Alt, S. Manz, M. Martinez-Dorantes, R. Reimann, S. Yoon, D. Meschede, M. Bienert, and G. Morigi, Phys. Rev. A **89**, 033404 (2014).
[31] Y. Zhu, Opt. Lett. **35**, 303 (2010).
[32] B. Zou and Y. Zhu, Phys. Rev. A **87**, 053802 (2013).
[33] H. S. Borges and C. J. Villas-Bôas, Phys. Rev. A **94**, 052337 (2016).
[34] A. Joshi and M. Xiao, Phys. Rev. Lett. **91**, 143904 (2003).
[35] X. Wei, J. Zhang, and Y. Zhu, Phys. Rev. A **82**, 033808 (2010).
[36] W. Chen, K. M. Beck, R. Bücker, M. Gullans, M. D. Lukin, H. Tanji-Suzuki, and V. Vuletić, Science **341**, 768 (2013).
[37] M. Albert, A. Dantan, and M. Drewsen, Nat. Photon. **5**, 633 (2011).
[38] A. E. B. Nielsen and J. Kerckhoff, Phys. Rev. A **84**, 043821 (2011).
[39] A. D. Boozer, A. Boca, R. Miller, T. E. Northup, and H. J. Kimble, Phys. Rev. Lett. **98**, 193601 (2007).
[40] M. Himsworth, P. Nisbet, J. Dilley, G. Langfahl-Klabes, and A. Kuhn, Appl. Phys. B **103**, 579 (2011).
[41] J. Sheng, Y. Chao, S. Kumar, H. Fan, J. Sedlacek, and J. P. Shaffer, Phys. Rev. A **96**, 033813 (2017).
[42] J. Li, Y. Qu, R. Yu, and Y. Wu, Phys. Rev. A **97**, 023826 (2018).
[43] C. J. Zhu, Y. P. Yang, and G. S. Agarwal, Phys. Rev. A **95**, 063842 (2017).
[44] M.-O. Pleinert, J. von Zanthier, and G. S. Agarwal, Optica **4**, 779 (2017).
[45] M.-O. Pleinert, J. von Zanthier, and G. S. Agarwal, Phys. Rev. A **97**, 023831 (2018).

[46] G. Yang, W.-j. Gu, G. Li, B. Zou, and Y. Zhu, Phys. Rev. A **92**, 033822 (2015).

[47] C. Hamsen, K. N. Tolazzi, T. Wilk, and G. Rempe, Nat. Phys. **14**, 885 (2018).

[48] R. B. Li, C. J. Zhu, L. Deng, and E. W. Hagley, Phys. Rev. A **92**, 043838 (2015).

[49] The probe field η is very weak so it can be treated as a perturbation to the Hamiltonian of the system.

[50] H. Chibani, Ph.D. thesis, Technische Universität München, 2016.

[51] The value of κ is several MHz, which can be realized in current experiments.